Influence of C-Doping on the B-11 and N-14 Quadrupole Coupling Constants in Boron-Nitride Nanotubes: A DFT Study

Mahmoud Mirzaei[a], Nasser L. Hadipour[a], and Mohammad Reza Abolhassani[b,c]

[a] Department of Chemistry, Tarbiat Modares University, P.O. Box 14115-175, Tehran, Iran
[b] Department of Physics, Tarbiat Modares University, Tehran, Iran
[c] Plasma Physics Research Center, Science and Research Campus, Islamic Azad University, P.O. Box 14515-775, Tehran, Iran

Reprint requests to Dr. N. L. H.; Fax: (+98) 21 8800-9730; E-mail: hadipour.n@gmail.com

Z. Naturforsch. **62a,** 56 – 60 (2007); received December 18, 2006

A computational study at the level of density functional theory (DFT) was carried out to investigate the influence of carbon doping (C-doping) on the ^{11}B and ^{14}N quadrupole coupling constants (C_Q) in the (6,0) single-walled boron-nitride nanotube (BNNT). To this aim, a 10 Å length of BNNT consisting of 24 B atoms and 24 N atoms was selected where the end atoms are capped by hydrogen atoms. To follow the purpose, six C atoms were doped instead of three B and three N atoms as a central ring in the surface of the C-doped BNNT. The calculated C_Q values for both optimized BNNT systems, raw and C-doped, reveal different electrostatic environments in the mentioned systems. It was also demonstrated that the end nuclei have the largest C_Q values in both considered BNNT systems.

Key words: C-Doping; Boron-Nitride; BNNT; Nanotube; Quadrupole Coupling Constant; DFT.

1. Introduction

Since the discovery of carbon nanotubes (CNTs) [1], many kinds of CNTs [2 – 4] have been studied. The properties of CNTs are dependent mainly on their chirality, therefore, controlling the synthesis of CNTs for special purposes is very difficult [5]. Replacing CNTs by non-carbon nanotubes, the properties of which are less dependent on their chirality, is a way to solve the problem. A good replacement is the boron-nitride nanotube (BNNT) [6], which is a semiconductor independent of chirality [7]. Furthermore, because, the electronegativity of N is larger than that of B, the non-equivalent ending nuclei cause electric polarization effects in the BNNTs which may suggest them for optoelectronic applications [8]. Boron and nitrogen are the neighbors of carbon in the periodic table, and the sum of the atomic numbers of B and N equals that of two carbon atoms. Therefore CNTs and BNNTs are similar to each other. The characteristic properties of BNNTs made them the subject of numerous studies [9 – 13].

Nuclear quadrupole resonance (NQR) spectroscopy characterizes the physical properties of matters [14]. Electric field gradient (EFG) tensors are very sensitive to the electrostatic environment at the sites of quadrupole nuclei with spin angular momenta greater than one-half, e. g. ^{11}B and ^{14}N. Experimentally, quadrupole coupling constants (C_Q) and asymmetry parameters (η_Q) are measured by NQR. However, because of the inhomogeneity of the electrostatic environment in nanotubes, performing experimental NQR studies on nanotubes is very difficult. On the other hand, high-level quantum chemical calculations can reproduce reliable NQR parameters [15, 16], therefore, performing such studies can help to predict NQR parameters in the nanotubes.

In the present work we study the influence of carbon doping (C-doping) on the ^{11}B and ^{14}N quadrupole coupling constants in the (6,0) single-walled BNNT with a tube length of 10 Å, the two ends of the tubes being capped by hydrogen atoms (see Fig. 1). To have a systematic interpretation of the purpose, two BNNTs were considered in the NQR calculations, the first model is a raw BNNT and the second one is a C-doped BNNT. Both model systems were first optimized, and then the NQR calculations were performed. To the best of our knowledge, there are no available NQR data for the considered model systems of BNNTs in the literature.

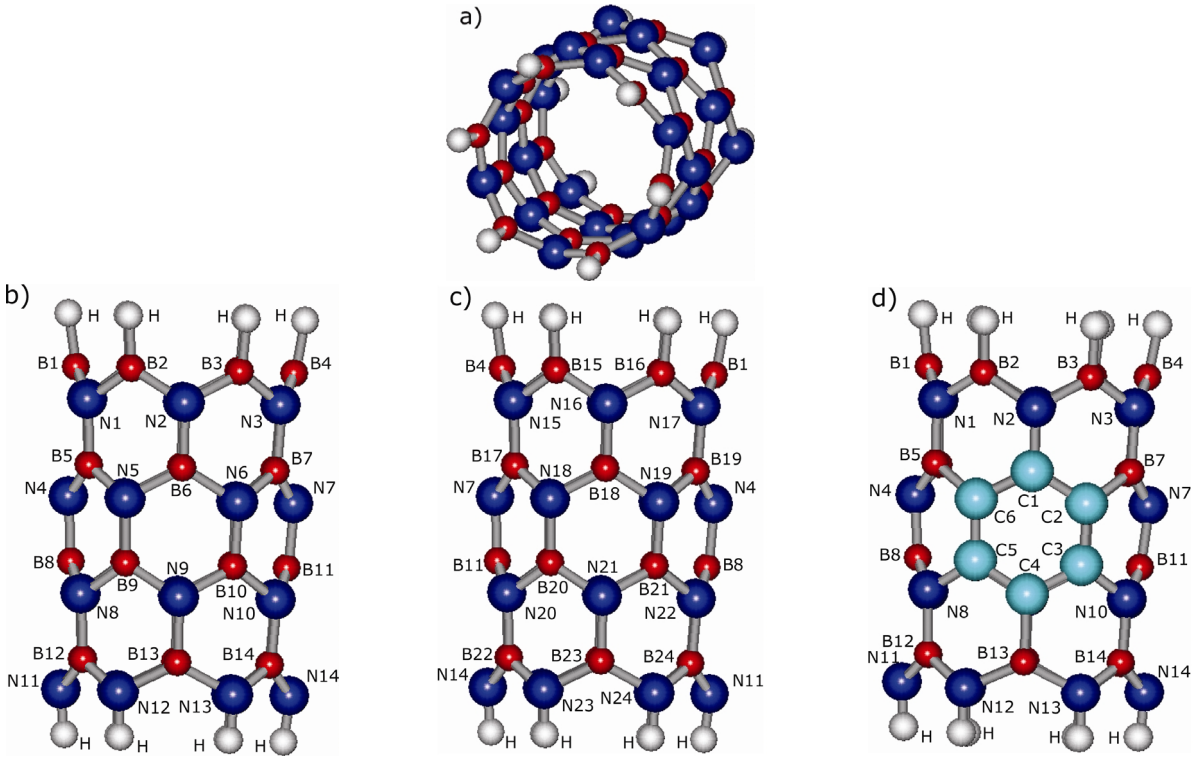

Fig. 1. a) The (6,0) single-walled BNNT in 3D view. b) The raw BNNT in 2D view, the front side. c) The raw BNNT in 2D view, the back side. d) The C-doped BNNT in 2D view, the front side. The back side is the same as in c.

Table 1. ^{11}B NQR Parameters. In each row, the values in brackets are for C-doped BNNT and those out of brackets are for raw BNNT.

Nucleus	C_Q (MHz)	η_Q
B1	4.07 [4.10]	0.30 [0.30]
B2	4.07 [3.90]	0.30 [0.35]
B3	4.06 [3.90]	0.30 [0.35]
B4	4.07 [4.10]	0.30 [0.30]
B5	3.22 [3.44]	0.08 [0.25]
B6	3.22 [—]	0.08 [—]
B7	3.22 [3.44]	0.08 [0.25]
B8	3.18 [3.22]	0.07 [0.16]
B9	3.18 [—]	0.07 [—]
B10	3.18 [—]	0.07 [—]
B11	3.18 [3.22]	0.07 [0.16]
B12	3.06 [2.99]	0.09 [0.07]
B13	3.06 [3.27]	0.09 [0.32]
B14	3.06 [3.00]	0.09 [0.07]
B15	4.07 [4.07]	0.30 [0.30]
B16	4.06 [4.07]	0.30 [0.30]
B17	3.22 [3.21]	0.08 [0.08]
B18	3.22 [3.21]	0.08 [0.08]
B19	3.22 [3.21]	0.08 [0.08]
B20	3.18 [3.16]	0.07 [0.08]
B21	3.18 [3.16]	0.07 [0.08]
B22	3.06 [3.07]	0.09 [0.08]
B23	3.06 [3.07]	0.09 [0.08]
B24	3.06 [3.07]	0.09 [0.08]

Table 2. ^{14}N NQR Parameters. In each row, the values in brackets are for C-doped BNNT and those out of brackets are for raw BNNT.

Nucleus	C_Q (MHz)	η_Q
N1	1.00 [1.11]	0.49 [0.41]
N2	1.00 [2.13]	0.50 [0.27]
N3	1.00 [1.11]	0.50 [0.41]
N4	1.09 [0.96]	0.10 [0.23]
N5	1.09 [—]	0.10 [—]
N6	1.09 [—]	0.09 [—]
N7	1.09 [0.96]	0.10 [0.23]
N8	1.18 [2.76]	0.08 [0.96]
N9	1.19 [—]	0.08 [—]
N10	1.19 [2.76]	0.08 [0.96]
N11	2.58 [2.73]	0.84 [0.77]
N12	2.58 [2.33]	0.84 [0.98]
N13	2.58 [2.33]	0.84 [0.98]
N14	2.58 [2.73]	0.84 [0.77]
N15	1.00 [0.99]	0.49 [0.56]
N16	1.00 [0.95]	0.50 [0.51]
N17	1.00 [0.99]	0.50 [0.56]
N18	1.09 [1.03]	0.10 [0.09]
N19	1.09 [1.03]	0.09 [0.09]
N20	1.18 [1.23]	0.08 [0.01]
N21	1.19 [1.23]	0.08 [0.01]
N22	1.19 [1.23]	0.08 [0.01]
N23	2.58 [2.55]	0.84 [0.84]
N24	2.58 [2.55]	0.84 [0.84]

The calculated C_Q and η_Q parameters are presented in Tables 1 and 2.

2. Computational Details

All quantum chemical calculations were performed at the level of the density functional theory (DFT) by the Gaussian 98 package of the program [17]. Two models of H-capped (6,0) single-walled BNNTs with a tube length of 10 Å were considered. Model one considers a raw BNNT and model two a C-doped BNNT (see Fig. 1). Both systems were firstly optimized at the level of the B3LYP [18, 19] method and 6-311G** standard basis set, and then the NQR calculations were performed on the optimized model systems at the level of the B3LYP method and the 6-311++G** standard basis set.

Experimentally the measurable NQR parameters are the quadrupole coupling constant (C_Q) and the asymmetry parameter (η_Q). C_Q refers to the interaction energy of the nuclear electric quadrupole moment (eQ) and the EFG tensors at the site of quadrupole nucleus. η_Q is defined as the EFG tensors deviation from cylindrical distribution at the site of quadrupole nucleus. The quantum chemical calculations yield the EFG tensors in the principal axis system (PAS) with the order $|q_{zz}| > |q_{yy}| > |q_{xx}|$, equations (1) and (2) are used to directly relate the calculated EFG tensors with the measurable parameters C_Q and η_Q. The standard Q values reported by Pyykkö [20] are employed in (1), $Q(^{11}\mathrm{B}) = 40.59$ mb and $Q(^{14}\mathrm{N}) = 20.44$ mb. Tables 1 and 2 exhibit the calculated NQR parameters for ^{11}B and ^{14}N, respectively.

$$C_Q\ (\mathrm{MHz}) = e^2 Q q_{zz} h^{-1}, \tag{1}$$

$$\eta_Q = |(q_{xx} - q_{yy})/q_{zz}| \quad (0 < \eta_Q < 1). \tag{2}$$

3. Results and Discussion

A DFT study was carried out to investigate the influence of C-doping on the quadrupole coupling constants of the ^{11}B and ^{14}N nuclei in the H-capped (6,0) single-walled BNNT. To this aim, two model systems of raw BNNT and C-doped BNNT were considered in the calculations (see Fig. 1). The raw system consists of 24 B atoms and 24 N atoms, whereas in the C-doped system, six C atoms are replaced instead of three N and three B atoms as a central ring in the surface of a tube. Firstly, the two model systems were optimized, and then the NQR calculations were carried out on the optimized structures (see Tables 1 and 2). The following text will discuss the calculated results of $C_Q(^{11}\mathrm{B})$ and $C_Q(^{14}\mathrm{N})$ in the two model systems separately.

3.1. The ^{11}B Quadrupole Coupling Constants

Table 1 presents the calculated NQR parameters (C_Q and η_Q) for ^{11}B in both model systems of raw and C-doped BNNTs. A quick look at the results reveals that C-doping in the tube significantly changes the electrostatic environment of the BNNT, as can easily be seen by the different $C_Q(^{11}\mathrm{B})$ and $\eta_Q(^{11}\mathrm{B})$ of various B nuclei in the two model systems. Furthermore, the EFG tensors at the sites of ^{11}B nuclei in the raw system do not feel equivalent electrostatic environments, as can be seen by their decreasing of $C_Q(^{11}\mathrm{B})$ values from the B-end to the N-end of the nanotube. This is because B and N have different electronegativities, that of N being larger than that of B. This yields an asymmetric charge distribution along the nanotube. Therefore, the atoms on each end have the largest C_Q values, which decrease along the tube to the opposite end. There are 24 B atoms in the raw BNNT system, and in the C-doped system three B atoms are replaced by C atoms. B1, B2, B3, B4, B15, and B16 are located in the B-end of the nanotube. In the raw system all mentioned nuclei feel a similar electrostatic environment, as can be easily seen in their calculated NQR parameters. However, in the C-doped system this similarity is perturbed and a different situation occurres for B-end nuclei. It is noteworthy that in this situation the nuclei in symmetric positions have still similar electrostatic environments, but different from the parameters of nuclei in other positions. Couples of B1/B4, B2/B3, and B15/B16 have similar NQR parameters, meaning that the ^{11}B EFG tensors at their sites feel similar electrostatic environments. Furthermore, the calculated parameters of B15 and B16 remained unchanged, while those of B2 and B3, which are in the neighbourhood of N2, which is directly chemically bound to C1, are significantly changed, and their $C_Q(^{11}\mathrm{B})$ are reduced by 0.17 MHz.

B5, B6, B7, B17, B18, and B19 is the next series of B nuclei which have a similar electrostatic environment in the raw system. In the C-doped system, B6 is replaced by C1, then B5 and B7 which are placed in the two neighbour sides of C1 and are directly chemically bound to C6 and C2, respectively, have similar NQR parameters but different from those in the raw system.

Their $C_Q(^{11}B)$ are increased by 0.22 MHz rather than the raw system, $r_{B-N} = 1.45$ Å and $r_{B-C} = 1.53$ Å. However, the $C_Q(^{11}B)$ of B17, B18, and B19 remained almost unchanged in the two model systems. B8, B9, B10, B11, B20, and B21 is the other series of nuclei which are in the same situation in the raw system, however, B9 and B10 are replaced by C5 and C3, respectively, in the C-doped system. The NQR parameters of the other B nuclei of this series do not show any significant changes. B12, B13, B14, B22, B23, and B24 is the last series of B nuclei in the considered BNNT model. B12 and B14 are in symmetric positions, and their electrostatic environment is almost the same, but their calculated NQR parameters are changed from the raw to the C-doped system. The values of $C_Q(^{11}B)$ are reduced by 0.06 MHz. However, the calculated NQR parameters of B22, B23, and B24 are almost the same in the two model systems. Similar to B5 and B7, B13 is directly chemically bound to C4, and its $C_Q(^{11}B)$ is increased by 0.21 MHz. The changes of $\eta_Q(^{11}B)$ almost agree with the changes of $C_Q(^{11}B)$ for various B nuclei in the considered BNNT model systems.

3.2. The ^{14}N Quadrupole Coupling Constants

Table 2 exhibits the calculated NQR parameters of ^{14}N nuclei in the raw and C-doped BNNT model systems. Similar to the B nuclei, $C_Q(^{14}N)$ decreases from the N-end to the B-end of the BNNT, which means that the nuclei at the ends of the BNNT are more active than those located in the other positions of the nanotube. There are four sets of N nuclei in the raw BNNT, whereas this similarity is perturbed by C-doping. N11, N12, N13, N14, N23, and N24 are N-end nuclei in the BNNT. They have similar NQR parameters in the raw model system, whereas this equivalent set of N nuclei is divided into 3 equivalent sets as N11/N14, N12/N13, and N23/N24 in the C-doped system. As can be seen in Table 2, $C_Q(^{14}N)$ of N12 and N13 is reduced by 0.25 MHz in the C-doped system, while the $C_Q(^{14}N)$ of N11 and N14 is increased by 0.15 MHz. This trend means that, regarding $C_Q(^{11}B)$ of B12, B13, and B14, N23 and N24 make stronger bonding with B12, B13, and B14, so the bonding of N11-B12 and also N14-B14 is weakened, therefore, for N11 and N14, the values of $C_Q(^{14}N)$ are increased and those of $\eta_Q(^{14}N)$ are decreased.

The next set of N nuclei in the considered system consists of N8, N9, N10, N20, N21, and N22, where N21 is replaced by C4 in the C-doped system. Although the mentioned nuclei have a similar electrostatic environment in the raw system, they lose this similarity in the C-doped system and are divided into two sets of nuclei. N8 and N10 are chemically bound to C5 and C3, respectively, $r_{C-N} = 1.43$ Å and $r_{B-N} = 1.45$ Å, and as a result their NQR parameters are significantly influenced by these bonds, the $C_Q(^{14}N)$ of N8 and N10 is increased by 1.58 MHz. N4, N5, N6, N7, N18, and N19 make the next set of N nuclei in the considered systems, where N5 and N6 are replaced by C6 and C2, respectively, in the C-doped system. N4/N7 and N18/N19 are those nuclei which are in symmetric positions in the C-doped system, and the influences on the NQR parameters are similar. The last set of N nuclei consists of N1, N2, N3, N15, N16, and N17, where N2 is chemically bound to C1 in the C-doped system and its $C_Q(^{14}N)$ increases by 1.13 MHz. The $C_Q(^{14}N)$ values of N1 and N3 are also increased by 0.11 MHz but those of N15, N16, and N17 remain almost unchanged in the two model systems. In agreement with the changes of $C_Q(^{14}N)$, the values of $\eta_Q(^{14}N)$ are also changed in the considered systems.

4. Concluding Remarks

Our work was a computational NQR study to investigate the influence of C-doping on the ^{11}B and ^{14}N quadrupole coupling constants in the two (6,0) BNNT model systems including raw and C-doped systems. The calculated parameters for the two systems show significant differences for some nuclei, while for some other nuclei no difference is observed. The following trends are concluded by this study. First, the raw BNNT system does not have similar NQR parameters because of the polarity of the ending nuclei. The values of $C_Q(^{11}B)$ are increased from the N-end to the B-end nuclei, and the values of $C_Q(^{14}N)$ are increased from the B-end to the N-end nuclei. Second, the NQR parameters of B9 and N5 can be considered as characteristic NQR values for long nanotubes. Third, the influence of C-doping on the C_Q parameters for those nuclei in neighbourhood is significant, while for the other ones it is almost negligible. The $C_Q(^{11}B)$ and $C_Q(^{14}N)$ values of those B and N nuclei which are directly chemically bound to the C atom are increased in the C-doped system.

[1] S. Iijima, Nature **354**, 56 (1991).
[2] H. S. Kang, J. Phys. Chem. B **110**, 4621 (2006).
[3] E. Zurek and J. Autscbach, J. Am. Chem. Soc. **126**, 13079 (2004).
[4] A. N. Enyashin, Yu. N. Makurin, and A. L. Ivanovskii, Carbon **42**, 2081 (2004).
[5] P. J. F. Harris, Carbon Nanotubes and Related Structures, Cambridge University Press, Cambridge 1999.
[6] A. Loiseau, F. Willaime, N. Demoncy, N. Schramcheko, G. Hug, C. Colliex, and H. Pascard, Carbon **36**, 743 (1998).
[7] X. Balasé, A. Rubio, S. G. Louie, and M. L. Cohen, Europhys. Lett. **28**, 335 (1994).
[8] P. Karl, E. J. Mele, and D. Tomanek, Phys. Rev. Lett. **85**, 1512 (2000).
[9] M.-D. Su, J. Phys. Chem. B **109**, 21647 (2005).
[10] S.-H. Jhi and Y.-K. Kwon, Phys. Rev. B **69**, 245407 (2004).
[11] M. Machado, P. Piquini, and R. Mota, Chem. Phys. Lett. **392**, 428 (2004).
[12] R. A. de la Concha and A. Loiseau, Phys. Rev. B **68**, 045425 (2003).
[13] J. Kongsted, A. Osted, L. Jensen, P.-O. Åstrand, and K. V. Mikkelsen, J. Phys. Chem. B **105**, 10243 (2001).
[14] T. P. Das and E. L. Han, Nuclear Quadrupole Resonance Spectroscopy, Academic Press, New York 1958.
[15] T. Partovi, M. Mirzaei, and N. L. Hadipour, Z. Naturforsch. **61a**, 383 (2006).
[16] M. Mirzaei and N. L. Hadipour, J. Phys. Chem. A **110**, 4833 (2006).
[17] M. J. Frisch, G. W. Trucks, H. B. Schlegel, G. E. Scuseria, M. A. Robb, J. R. Cheeseman, V. G. Zakrzewski, J. A. Montgomery, Jr., R. E. Stratmann, J. C. Burant, S. Dapprich, J. M. Millam, A. D. Daniels, K. N. Kudin, M. C. Strain, O. Farkas, J. Tomasi, V. Barone, M. Cossi, R. Cammi, B. Mennucci, C. Pomelli, C. Adamo, S. Clifford, J. Ochterski, G. A. Petersson, P. Y. Ayala, Q. Cui, K. Morokuma, D. K. Malick, A. D. Rabuck, K. Raghavachari, J. B. Foresman, J. Cioslowski, J. V. Ortiz, A. G. Baboul, B. B. Stefanov, G. Liu, A. Liashenko, P. Piskorz, I. Komaromi, R. Gomperts, R. L. Martin, D. J. Fox, T. Keith, M. A. Al-Laham, C. Y. Peng, A. Nanayakkara, C. Gonzalez, M. Challacombe, P. M. W. Gill, B. Johnson, W. Chen, M. W. Wong, J. L. Andres, C. Gonzalez, M. Head-Gordon, E. S. Replogle, and J. A. Pople, Gaussian 98, Revision A.7, Gaussian, Inc., Pittsburgh, PA 1998.
[18] A. D. Becke, J. Chem. Phys. **98**, 5648 (1993).
[19] C. Lee, W. Yang, and R. G. Parr, Phys. Rev. B **37**, 785 (1988).
[20] P. Pyykkö, Mol. Phys. **99**, 1617 (2001).